On the selection principle for viscous fingering in porous media

By Y. C. YORTSOS[1] and D. SALIN[2]

[1]Mork Family Department of Chemical Engineering and Materials Science, University of Southern California, Los Angeles, CA 90089-1211, USA

[2]Laboratoire FAST, Fluides Automatique et Systèmes Thermiques, Université P. M. Curie, Université Paris Sud, CNRS UMR 7608 Bât. 502, Campus Universitaire, F-91405 Orsay Cedex, France

Viscous fingering in porous media at large Péclet numbers is subject to an unsolved selection problem, not unlike the Saffman–Taylor problem. The mixing zone predicted by the entropy solution is found to spread much faster than is observed experimentally or from fine-scale numerical simulations. In this paper we apply a recent approach by Menon & Otto (*Commun. Math. Phys.*, vol. 257, 2005, p. 303), to develop bounds for the mixing zone. These give growth velocities smaller than the entropy solution result $(M - 1/M)$. In particular, for an exponential viscosity-concentration mixing rule, the mixing zone velocity is bounded by $(M - 1)^2/(M \ln M)$, which is smaller than $(M - 1/M)$. An extension to a porous medium with an uncorrelated random heterogeneity is also given.

1. Introduction

Viscous fingering in miscible displacements in porous media has been extensively investigated in the past. The origin of the instability was discussed in pioneering works by Saffman & Taylor (1958), in the context of immiscible displacement in a Hele-Shaw cell, and by Wooding (1969) in the context of miscible displacement, also in a Hele-Shaw cell. Viscous fingering in porous media has been extensively analysed (e.g. see reviews by Homsy 1987; Tanveer 2000 and a more recent analysis by Yang, Yortsos & Salin 2002). The instability is long-wave, developing, in the absence of gravity, when the ratio of viscosities between displaced and displacing fluids is greater than one. Gravity also exerts a long-wave effect, and can be stabilizing or destabilizing, depending on the direction of the displacement and the density of the fluids involved. A number of experimental, theoretical and numerical works have recently been devoted to the understanding of various aspects of the instability (Manickam & Homsy 1991; Zimmerman & Homsy 1992; Loggia *et al.* 1995; Tanveer 2000; Smirnov *et al.* 2005). Despite the considerable work done, however, an important issue has remained unresolved so far, namely the selection of the spreading of the mixing zone.

Consider miscible displacement in the absence of gravity in a two-dimensional porous medium of a rectilinear geometry (dimensions L and H, respectively, e.g. see figure 1): fluid 1, initially in the porous medium, is displaced at constant injection rate q by fluid 2, miscible with the former, and with lower viscosity ($\mu_1 > \mu_2$). The resulting unstable displacement will be parameterized using the local concentration c, where $c = 0$ corresponds to the initial fluid and $c = 1$ to the injected. Following the onset of instability, a mixing zone develops. Under conditions of high Péclet number ($Pe \gg 1$), where convection dominates, the mixing zone spreads linearly in
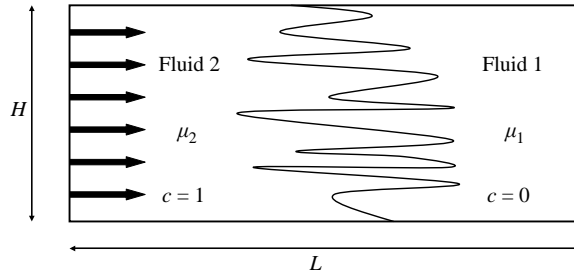
FIGURE 1. Schematic of the problem considered. Fluid 2 miscibly displaces a more viscous fluid 1 in the direction indicated. The geometry of the displacement is rectilinear. Viscous fingers develop as a result of the instability.

time, the leading edge traveling asymptotically with velocity v_1 and the trailing edge with velocity v_2. Determining the two velocities is important for a number of reasons, including an understanding of the efficiency of the displacement. However, their precise determination has so far eluded past investigators.

When the instability has fully developed, the displacement reaches an asymptotic regime, which Yortsos (1995) termed as the state of transverse flow equilibrium (TFE) (generalizing the earlier terminology of vertical flow equilibrium (VFE), e.g. Lake 1989). In this regime, the flow is essentially parallel, the pressure gradient in the flow direction x being independent of the transverse coordinate y to leading-order in the variable H/L. (Typically, in reservoir-engineering-related problems y is the vertical coordinate, hence the VFE terminology). In his seminal paper, in the context of gravity-driven miscible instability in a Hele-Shaw cell, Wooding (1969) also proposed a corresponding regime (discussed further below). Under these conditions, it was shown by Yortsos (1995) that to leading-order the streamwise velocity u is an explicit function of the mobility, given in dimensionless notation by

$$u = \frac{k\lambda}{\displaystyle\int_0^1 k\lambda \, dy} \tag{1.1}$$

where k is a normalized permeability, lengths have been scaled with the thickness H, and we have defined the dimensionless mobility

$$\lambda(c) = \frac{\mu_1}{\mu(c)}. \tag{1.2}$$

The latter is a function of the local concentration field c, such that $\lambda(0) = 1$ and $\lambda(1) = M > 1$, where M is the end-point viscosity ratio. For future reference we note the exponential model

$$\lambda(c) = \exp(Rc) \tag{1.3}$$

where $R = \ln M$. In the above, we have assumed that the medium is in general heterogeneous, $k = k(\mathbf{x})$. In the sections that follow we will restrict our attention to a homogeneous medium and take $k = 1$, however. An extension to the heterogeneous case will be briefly presented at the end of the paper. The problem is completed with mass balances for the solute and the solvent

$$\frac{\partial c}{\partial t} + \left(\frac{\lambda(c)}{\displaystyle\int_0^1 \lambda(c) \, dy} \right) \frac{\partial c}{\partial x} + w\frac{\partial c}{\partial y} = \frac{1}{Pe}\nabla^2 c \tag{1.4}$$
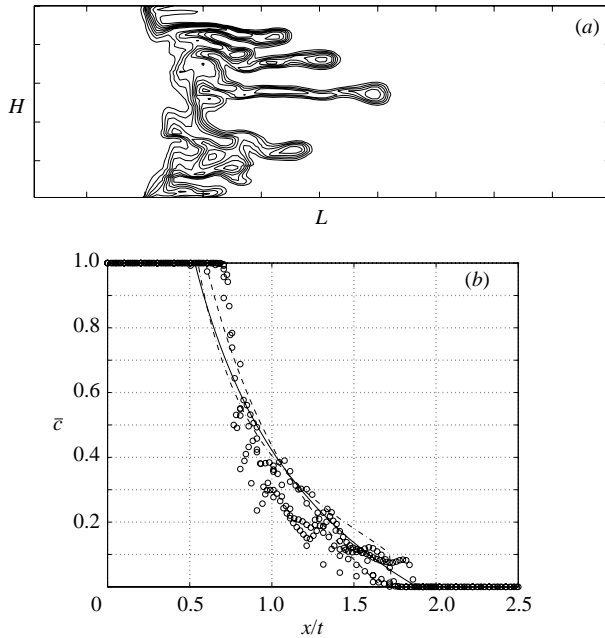
FIGURE 2. (*a*) A typical viscous fingering pattern (numerical simulations) under conditions of transverse flow equilibrium (TFE) and for a viscosity ratio $M = 10$. The pattern has the typical features of the viscous instability. Lines correspond to different iso-concentration contours. (*b*) Transverse-average concentration profiles of (*a*), versus the velocity of average concentration, for $M = 10$. The open circles correspond to different numerical simulation runs. The lines close to the data correspond to a proposed model (from Yang *et al.* (2002)).

and

$$\frac{\partial u}{\partial x} + \frac{\partial w}{\partial y} = 0 \tag{1.5}$$

where w is the transverse velocity and Pe denotes the Péclet number.

Yang *et al.* (2002) studied the linear stability of the TFE formulation and showed that it contains both the long-wave fingering instability and the stabilizing influence of dispersion, as expected, thus representing a good limiting model of the problem. Yang & Yortsos (1998) and Yang *et al.* (2002) explored numerically the properties of the developed instability and showed that it displays typical aspects of viscous fingering patterns, including tip splitting, shielding and finger coalescence (Homsy 1987) (e.g. see figure 2). In particular, the simulations of Yang *et al.* (2002) show that the resulting mixing zone is largest under TFE conditions, hence any estimates of its length will also bound the mixing zone length under other than TFE conditions.

2. The transverse-averaged equation and the entropy solution

In conjunction with the TFE expression (1.1) and the continuity equation (1.5), equation (1.4) can be integrated over the transverse coordinate y to give the transverse-average equation

$$\frac{\partial \bar{c}}{\partial t} + \frac{\partial}{\partial x}\left(\frac{\int_0^1 \lambda(c)c\,\mathrm{d}y}{\int_0^1 \lambda(c)\,\mathrm{d}y}\right) = \frac{1}{Pe}\frac{\partial^2 \bar{c}}{\partial x^2} \tag{2.1}$$

Y. C. Yortsos and D. Salin

where the overbar denotes average across y. To proceed further, the 'fractional flow' function in the convective term on the left-hand side

$$F(\bar{c}) = \overline{uc} = \frac{\displaystyle\int_0^1 \lambda(c) c \, dy}{\displaystyle\int_0^1 \lambda(c) \, dy} \quad (2.2)$$

must be expressed. A tempting, but as will turn out naïve, choice is to assume that in the fingering pattern all fingered regions have the same maximum local concentration $c = 1$ and all non-fingered regions the same minimum concentration $c = 0$. This assumption is based on neglecting local mixing due to molecular diffusion, thus of any zone of graded mobility. Then, the fractional flow becomes

$$F_n(C) = \frac{MC}{(MC + 1 - C)}. \quad (2.3)$$

In the fingering case ($M > 1$), this function is convex. Using (2.3) in (2.1) we obtain

$$\frac{\partial \bar{c}}{\partial t} + \frac{\partial}{\partial x} \left(\frac{M\bar{c}}{M\bar{c} + 1 - \bar{c}} \right) = \frac{1}{Pe} \frac{\partial^2 \bar{c}}{\partial x^2}. \quad (2.4)$$

Its solution in the high-Pe limit, with initial condition $\bar{c} = 0$ for $x > 0$ and $\bar{c} = 1$ for $x < 0$, is the rarefaction

$$\bar{c} = 1 \quad \text{for} \quad x < t/M, \quad \bar{c} = 0 \quad \text{for} \quad x > tM \quad (2.5)$$

and

$$\bar{c} = \frac{1}{M-1} \left[\sqrt{\frac{Mt}{x}} - 1 \right] \quad \text{for} \quad t/M < x < tM. \quad (2.6)$$

Equation (2.6) states that in the entropy solution, the mixing zone spreads convectively, with a leading velocity equal to M and a trailing velocity equal to $1/M$.

Experiments and numerical simulations of the full problem, including in the TFE regime, however, show conclusively that the true leading velocity is smaller than M and that the trailing-edge velocity is larger than $1/M$. A number of empirical models have been proposed to reconcile this behaviour (Koval 1963; Fayers 1988; Fayers, Jouaux & Tchelepi 1994; Todd & Longstaff 1972). For example, Koval (1963) postulated empirically that (2.3) is valid, provided that the end-point viscosity ratio M is replaced by an effective viscosity ratio M_{eff}, corresponding to an effective concentration in the fingered region $c_{eff} = 0.26$ to reflect local mixing, which even under high-Pe conditions cannot be neglected. A similar approach was used by Todd & Longstaff (1972). Yang *et al.* (2002) extensively reviewed these approaches and proposed semi-empirical models of their own. Despite the fact that such models appear to work in practice, a theoretical justification is yet to be obtained, however.

The situation is somewhat analogous to the Saffman & Taylor (1958) (ST) selection problem for viscous fingers in a Hele-Shaw cell: it is not difficult to show that in the TFE limit, the fractional flow function corresponding to the ST problem is the same as (2.3), with the understanding that it should be further considered in the limit $M \gg 1$. As is well known, in the absence of interfacial tension the ST finger selected is not the energetically more favourable, namely the one corresponding to the rarefaction (2.6) with an infinitely fast tip and a vanishing small thickness, but rather one that moves with velocity 2 and has a thickness of $1/2$. Finding the selection rule

in the ST problem remained unresolved for several decades, until it was formulated by a number of authors as a problem in asymptotics of all orders (Pelce 1988). To our knowledge, such an analogy has not yet been carried over to the miscible viscous fingering problem.

In a recent paper, Menon & Otto (2005) addressed the related problem of the Rayleigh–Taylor instability in a porous medium, which is the problem studied in a Hele-Shaw cell by Wooding (1969). These authors also focused attention on the TFE regime, using equations developed by Wooding. The corresponding expression for the streamwise velocity is

$$u = g_x \left[\rho(c) - \int_0^1 \rho(c) \, dy \right] \tag{2.7}$$

which is the equivalent to (1.1), and where g_x is the acceleration due to gravity in the direction of displacement. Consider next that the density is a linear function of the local concentration, and further take $g_x \dot{\rho} = -1$, which will induce instability when x is in the direction opposite to gravity. Here, $\dot{\rho} > 0$ is the derivative of the density with respect to concentration. Then, (2.7) becomes $u = \bar{c} - c$. The counterpart of equation (1.4) is now

$$\frac{\partial c}{\partial t} + [\bar{c} - c]\frac{\partial c}{\partial x} + w\frac{\partial c}{\partial y} = \frac{1}{Pe}\nabla^2 c \tag{2.8}$$

and the equation corresponding to (2.4) is

$$\frac{\partial \bar{c}}{\partial t} + \frac{\partial}{\partial x}(\bar{c}^2 - \bar{c}) = \frac{1}{Pe}\frac{\partial^2 \bar{c}}{\partial x^2}. \tag{2.9}$$

As before, the 'fractional flow' in the naïve approach ($\bar{c}^2 = \bar{c}$) is

$$F_g(C) = C^2 - C, \tag{2.10}$$

the hyperbolic equation in the high-Pe limit under this condition is

$$\frac{\partial \bar{c}}{\partial t} + \frac{\partial}{\partial x}(\bar{c}^2 - \bar{c}) = 0 \tag{2.11}$$

and the entropy solution is the rarefaction:

$$\bar{c} = 0 \quad \text{for} \quad x < -t, \quad \bar{c} = 1 \quad \text{for} \quad x > t \tag{2.12}$$

and

$$\bar{c} = \frac{1}{2}\left[1 + \frac{x}{t}\right] \quad \text{for} \quad -t < x < t. \tag{2.13}$$

This solution predicts a mixing zone that grows with a dimensionless velocity of 2. As in the viscous fingering case, however, this rate of growth overpredicts the true spreading, where the zone grows with dimensionless velocity 1. Menon & Otto (2005) made a fundamental breakthrough by showing that, in fact, the corresponding front velocities of the full problem cannot exceed the value of one half (hence, the mixing zone grows with a velocity not greater than one), as described below.

3. The Menon & Otto (2005) approach to the Wooding instability

The ingenious argument of Menon & Otto (2005) is based on bounding the solution both from above and from below by functions which propagate at a dimensionless speed of one half. An upper-bound solution was constructed by defining $c^*(t, x)$,
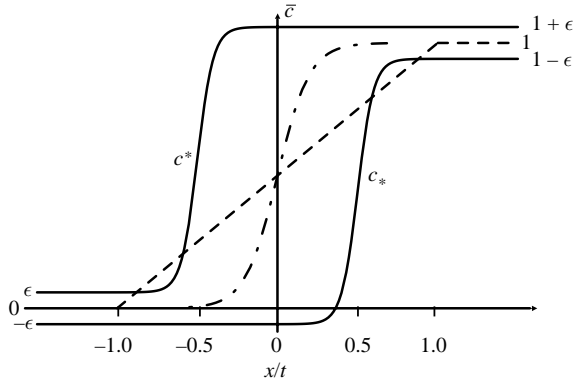
FIGURE 3. Transverse-average concentration profiles in the Rayleigh–Taylor instability in a porous medium, considered by Menon & Otto (2005). Shown are the upper and lower bounds, c^* and c_*, respectively. The dashed line is the entropy solution (2.13). The true solution is schematically shown by the dash-dot line.

which solves the Burgers' equation

$$\frac{\partial c^*}{\partial t} - \frac{\partial}{\partial x}\left(\frac{c^{*2}}{2}\right) = \frac{1}{Pe}\frac{\partial^2 c^*}{\partial x^2} \qquad (3.1)$$

subject to $c^* = 1 + \epsilon$ and $c^* = \epsilon$ at $\pm\infty$, where $0 < \epsilon \ll 1$. Equation (3.1) admits a travelling wave solution propagating at the constant speed

$$v_{g,\epsilon} = -\tfrac{1}{2} - \epsilon \qquad (3.2)$$

where we used subscript g to indicate the gravity instability problem. Menon & Otto (2005) used the maximum principle, by comparing the solution of (3.1) with that of the full problem (2.8), to show that c^* is an upper bound to the actual value (see figure 3). It follows that the downwards spreading of the mixing zone cannot travel faster than the velocity (3.2), which in the limit $\epsilon \to 0$ is in absolute value equal to one half.

Likewise, they constructed the lower bound by defining

$$\frac{\partial c_*}{\partial t} + \frac{\partial}{\partial x}\left(\frac{(1 - c_*)^2}{2}\right) = \frac{1}{Pe}\frac{\partial^2 c_*}{\partial x^2} \qquad (3.3)$$

subject to the boundary conditions $c_* = 1 - \epsilon$ and $c_* = -\epsilon$ at $\pm\infty$. A solution of (3.3) is again a travelling wave, now propagating at the speed

$$v_g^\epsilon = \tfrac{1}{2} + \epsilon. \qquad (3.4)$$

Again application of the maximum principle Menon & Otto (2005) shows that c_* is a lower bound to the full solution (figure 3), hence the upwards spreading of the mixing zone cannot travel with a velocity larger than v_g^ϵ, which in the small-ϵ limit reduces to one half.

4. Bounds on the viscous fingering instability

Motivated by Menon & Otto's work we apply the same arguments in order to bound the mixing zone growth in the viscous fingering case. Because of the presence of the transverse-averaged term in (2.1), however, we need to proceed somewhat
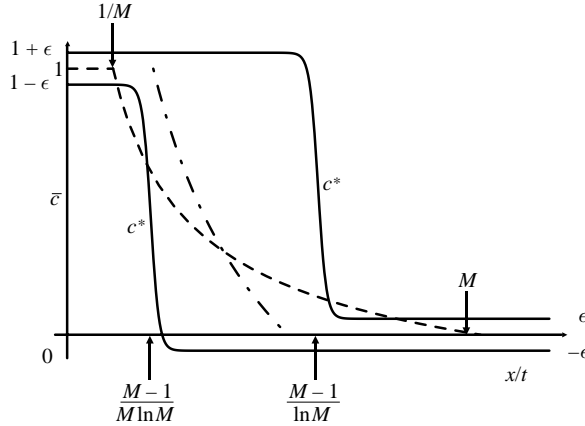
FIGURE 4. Transverse-average concentration profiles in the viscous fingering instability in a porous medium, considered in this paper. Shown are the upper and lower bounds, c^* and c_*, respectively. The dashed line is the entropy solution (2.6). The true solution is schematically shown by the dash-dot line.

differently. First, we note that

$$1 < \int_0^1 \lambda(c) \, dy < M. \tag{4.1}$$

Thus, we can construct an upper bound by defining

$$\frac{\partial c^*}{\partial t} + \lambda(c^*) \frac{\partial c^*}{\partial x} = \frac{1}{Pe} \frac{\partial^2 c^*}{\partial x^2} \tag{4.2}$$

subject to $c^* = \epsilon$ and $c^* = 1 + \epsilon$ at $\pm\infty$, where $0 < \epsilon \ll 1$. This comparison equation is obtained from (1.4) by setting $c = 0$ in the integral of the mobility function in the second term on the left-hand side. Equation (4.2) admits the travelling wave solution

$$\int_\epsilon^{c^*} \lambda(c) \, dc - v_v^\epsilon(c^* - \epsilon) = \frac{1}{Pe} \frac{\partial c^*}{\partial x} \tag{4.3}$$

which can be further integrated into an explicit form, if necessary. In the limit of high Péclet numbers, of interest in this paper, this solution is a shock connecting the upstream value $c^* = 1 + \epsilon$ to the downstream value $c^* = \epsilon$ (figure 4). The corresponding velocity is obtained by evaluating (4.3) at $c^* = 1 + \epsilon$ to find

$$v_v^\epsilon = \int_\epsilon^{1+\epsilon} \lambda(c) \, dc. \tag{4.4}$$

As shown below, c^* bounds the actual solution from above, hence the leading edge cannot travel faster than the velocity (4.4). For the exponential viscosity model (1.3), and in the limit of small ϵ, equation (4.4) further implies

$$v_v^0 = \frac{M - 1}{\ln M}. \tag{4.5}$$

This upper bound clearly satisfies $1 < v_v^0 < M$ (see also figure 5), thus demonstrating a slowdown of the true solution, compared to the naïve one, due to transverse mixing
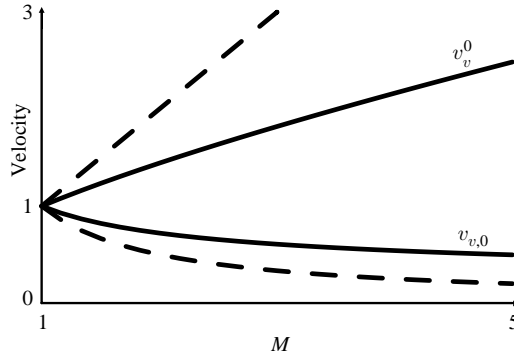
FIGURE 5. The variation of the velocities of the trailing and leading edges of the mixing zone in the viscous fingering problem, as a function of the viscosity ratio for an exponential viscosity profile. Solid line: the upper and lower bound solutions. Dashed line: the entropy solutions.

and diffusion. For a more general mobility function,

$$v_v^0 = \int_0^1 \lambda(c)\,dc.$$

To derive a lower bound, we define

$$\frac{\partial c_*}{\partial t} + \frac{\lambda(c_*)}{M}\frac{\partial c_*}{\partial x} = \frac{1}{Pe}\frac{\partial^2 c_*}{\partial x^2} \tag{4.6}$$

subject to $c^* = -\epsilon$ and $c_* = 1 - \epsilon$ at $\pm\infty$, where $0 < \epsilon \ll 1$. This comparison equation is obtained from (1.4) by setting $c = 1$ in the integral of the mobility function in the second term on the left-hand side. In the large time limit, equation (4.6) admits a travelling wave solution

$$\frac{\displaystyle\int_{-\epsilon}^{c_*} \lambda(c)\,dc}{M} - v_{v,\epsilon}(c_* + \epsilon) = \frac{1}{Pe}\frac{\partial c^*}{\partial x} \tag{4.7}$$

which can be further integrated into an explicit form, if needed. Again, in the limit of high Péclet numbers, of interest in this paper, this solution is a shock connecting the upstream value $1 - \epsilon$ to the downstream value $-\epsilon$ (figure 4). Its velocity is obtained by evaluating (4.7) at $c^* = 1 - \epsilon$ to yield

$$v_{v,\epsilon} = \frac{\displaystyle\int_{-\epsilon}^{1-\epsilon} \lambda(c)\,dc}{M}. \tag{4.8}$$

The function c_* bounds the actual solution from below, as will be shown later, hence the trailing edge cannot travel slower than the value given by (4.8). For example, for the exponential viscosity model (1.3) and in the limit of small ϵ, equation (4.8) leads to

$$v_{v,0} = \frac{M - 1}{M \ln M}. \tag{4.9}$$

This lower bound to the trailing velocity clearly satisfies $1/M < v_{v,0} < 1$ (see also figure 5). Again, for a more general mobility profile we should use

$$v_{v,0} = \frac{\int_0^1 \lambda(c)\,\mathrm{d}c}{M},$$

instead. The above show that for the exponential model, the mixing zone length cannot spread faster than $[(M-1)^2/(M \ln M)t]$, namely with velocity $(M-1)^2/(M \ln M)$ smaller than the naïve $(M - 1/M)$. Analogous results hold for the more general viscosity–concentration relation.

4.1. *Proofs*

To prove that c^* is an upper bound, we repeat the argument of Menon & Otto (2005) rephrased as follows. We subtract (1.4) from (4.2) and rearrange:

$$\frac{\partial \theta}{\partial t} + \left(\frac{\lambda(c^*) - \lambda(c)}{\int_0^1 \lambda(c)\,\mathrm{d}y} \right) \frac{\partial c^*}{\partial x} + \frac{\lambda(c)}{\int_0^1 \lambda(c)\,\mathrm{d}y} \frac{\partial \theta}{\partial x} + w \frac{\partial \theta}{\partial y} - \frac{1}{Pe} \nabla^2 \theta = \left(\frac{\lambda(c^*)}{\int_0^1 \lambda(c)\,\mathrm{d}y} - \lambda(c^*) \right) \frac{\partial c^*}{\partial x} \tag{4.10}$$

where we define $\theta = c^* - c$. We note that due to (4.1) the second term on the right-hand side of (4.10) is positive. Also, as $\theta \to 0$, the second term on the left-hand side becomes proportional to θ,

$$\frac{\lambda(c^*) - \lambda(c)}{\int_0^1 \lambda(c)\,\mathrm{d}y} \to \frac{\lambda'(\tilde{c})}{\int_0^1 \lambda(c)\,\mathrm{d}y} \theta,$$

where $\tilde{c}$ is between c^* and c. Menon & Otto (2005) applied the maximum principle to a similar equation, and showed that if $\theta > 0$ at $t = 0$, it remains positive at all times. The same argument carries through to equation (4.10). It relies on showing that $\theta \leqslant 0$ cannot be a minimum, and it is based on the fact that in that limit, the left-hand side tends to $-(1/Pe)\nabla^2 \theta$, and the right-hand side is positive. Both these conditions are satisfied in equation (4.10), hence we conclude that indeed c^* is an upper bound.

A similar analysis applies for the lower bound. Subtracting (4.6) from (1.4) leads to the following equation corresponding to (4.10):

$$\frac{\partial \theta}{\partial t} + \left(\frac{\lambda(c) - \lambda(c_*)}{\int_0^1 \lambda(c)\,\mathrm{d}y} \right) \frac{\partial c_*}{\partial x} + \frac{\lambda(c)}{\int_0^1 \lambda(c)\,\mathrm{d}y} \frac{\partial \theta}{\partial x} + w \frac{\partial \theta}{\partial y} - \frac{1}{Pe} \nabla^2 \theta = \left(\frac{\lambda(c^*)}{M} - \frac{\lambda(c^*)}{\int_0^1 \lambda(c)\,\mathrm{d}y} \right) \frac{\partial c^*}{\partial x} \tag{4.11}$$

where we define $\theta = c - c_*$. For the same reasons as above, $\theta > 0$, hence c_* is a lower bound to c.

4.2. *The weak-instability limit*

For completeness, it is worth noting that in the weak-instability limit, the viscous problem becomes identical to the one analysed by Menon & Otto (2005). Indeed, if $\hat{\lambda} = M - 1$ is small,

$$\lambda \approx 1 + (M - 1)c \tag{4.12}$$

in which case equation (1.4) becomes

$$\frac{\partial c}{\partial t} + (1 + (M-1)[c - \bar{c}])\frac{\partial c}{\partial x} + w\frac{\partial c}{\partial y} = \frac{1}{Pe}\nabla^2 c. \tag{4.13}$$

Subject to a change in coordinates and a rescaling, this is identical to the gravity problem discussed in Menon & Otto (2005). Proceeding as before it is not difficult to show that the leading-edge velocity is bounded above by $(M+1)/2 < M$ and the trailing-edge velocity bounded below by $(3-M)/2 > 1/M$. Both expressions $(M+1)/2$ and $(3-M)/2$ are asymptotic limits of (4.5) and (4.9) when $M-1 \ll 1$.

4.3. *Extension to heterogeneous media*

The above can be extended to the fingering problem in certain classes of heterogeneous media. We will proceed with the assumption of uncorrelated random heterogeneity and take $\int_0^1 k\,dy = 1$. We will now construct an upper bound by defining

$$\frac{\partial c^*}{\partial t} + k_u\lambda(c^*)\frac{\partial c^*}{\partial x} = \frac{1}{Pe}\frac{\partial^2 c^*}{\partial x^2} \tag{4.14}$$

subject to $c^* = \epsilon$ and $c^* = 1 + \epsilon$ at $\pm\infty$, where $0 < \epsilon \ll 1$. The parameter k_u is determined by considering the counterpart of (4.10), which here is

$$\frac{\partial \theta}{\partial t} + k\left(\frac{\lambda(c^*) - \lambda(c)}{\int_0^1 k\lambda(c)\,dy}\right)\frac{\partial c^*}{\partial x} + \frac{k\lambda(c)}{\int_0^1 k\lambda(c)\,dy}\frac{\partial \theta}{\partial x} + w\frac{\partial \theta}{\partial y} - \frac{1}{Pe}\nabla^2\theta$$

$$= \left(\frac{k\lambda(c^*)}{\int_0^1 k\lambda(c)\,dy} - k_u\lambda(c^*)\right)\frac{\partial c^*}{\partial x}. \tag{4.15}$$

Following the same rationale as in the homogeneous case, it is not difficult to show that we must require

$$\frac{k\lambda(c^*)}{\int_0^1 k\lambda(c)\,dy} - k_u\lambda(c^*) < 0,$$

which suggests the choice

$$k_u = \max\frac{k}{\int_0^1 k\lambda(c)\,dy}.$$

This is always satisfied by $k_u = k_{max}$. Then, by proceeding as previously, we will have, e.g. for the exponential model,

$$v_v^0 = k_{max}\frac{(M-1)}{\ln M}. \tag{4.16}$$

The corresponding lower bound is defined as the solution of

$$\frac{\partial c_*}{\partial t} + \frac{k_l\lambda(c_*)}{M}\frac{\partial c_*}{\partial x} = \frac{1}{Pe}\frac{\partial^2 c_*}{\partial x^2} \tag{4.17}$$

subject to $c^* = -\epsilon$ and $c_* = 1 - \epsilon$ at $\pm\infty$, where $0 < \epsilon \ll 1$. The constant k_l is determined by considering the counterpart of (4.11)

$$\frac{\partial \theta}{\partial t} + k \left(\frac{\lambda(c) - k\lambda(c_*)}{\displaystyle\int_0^1 k\lambda(c)\, dy} \right) \frac{\partial c_*}{\partial x} + \frac{k\lambda(c)}{\displaystyle\int_0^1 k\lambda(c)\, dy} \frac{\partial \theta}{\partial x} + w\frac{\partial \theta}{\partial y} - \frac{1}{Pe}\nabla^2\theta$$

$$= \left(\frac{k_l\lambda(c^*)}{M} - \frac{k\lambda(c^*)}{\displaystyle\int_0^1 k\lambda(c)\, dy} \right) \frac{\partial c^*}{\partial x}. \quad (4.18)$$

Now, the required condition is

$$\frac{k_l\lambda(c^*)}{M} - \frac{k\lambda(c^*)}{\displaystyle\int_0^1 k\lambda(c)\, dy} < 0,$$

which suggests

$$k_l = M \min \frac{k}{\displaystyle\int_0^1 k\lambda(c)\, dy},$$

and which is always satisfied by $k_l = k_{min}$. Proceeding as previously, we will have for the exponential model

$$v_{v,0} = k_{min} \frac{(M-1)}{M \ln M}. \quad (4.19)$$

Combining the two expressions (4.16) and (4.19) we see that for the exponential model, the spreading velocity of the mixing zone is bounded by $H(M-1)^2/(M \ln M)$, where the heterogeneity factor is $H = (Mk_{max} - k_{min})/(M-1)$. The result reduces to the previous one for the homogeneous case and to the expected velocity $k_{max} - k_{min}$ in the passive tracer case ($M = 1$).

5. Concluding remarks

In this paper we provide bounds on the problem of viscous fingering in porous media, and specifically on the leading- and trailing-edge velocities of the mixing zone. These bounds show that the actual solution does not grow as fast as predicted by the naïve solution of the transverse-averaged equations, based on the entropy solution of the resulting hyperbolic equation. This result is consistent with experimental studies and fine-scale numerical simulations in viscous fingering, and it is the first time that it has been proved rigorously. Whether these bounds are tight is not known, however. It is conceivable that tighter bounds do exist.

Although bounding the concentration profile, the solutions derived do not provide useful expressions for its details. Thus, they are unable to prove or disprove the validity of the typical approximations made, e.g. by Todd & Longstaff (1972), in which the fractional flow expression (2.3) is used for the transverse-average concentration, but with an appropriately adjusted effective viscosity ratio $M_{eff} < M$. Additional work in this direction is necessary. On the other hand, they provide a rigorous foundation that explains the retardation of the leading edge through transverse mixing.

The failure of the entropy solution to describe the actual evolution of the transversely averaged profile was observed before in a number of previous applications involving parallel flow. For example, Yang & Yortsos (1998) and Shariati *et al.* (2004) discussed this inadequacy in the context of Stokes flow between two parallel plates, and for a number of viscosity profiles. In particular, the latter study suggested that higher-dimensionality phenomena at the front cannot be captured by simple transverse averaging, which reduces the dimensionality of the problem. Non-classical shocks of the type introduced by Lefloch (2002) could potentially reconcile this problem.

REFERENCES

Fayers, F. J. 1988 An approximate model with physically interpretable parameters for representing viscous fingering. *SPE Reservoir Engng* **5**, 551–558.

Fayers, F. J., Jouaux, F. & Tchelepi, H. A. 1994 An improved macroscopic model for viscous fingering and its validation for 2D and 3D Flows – I. Non-gravity flows. *In Situ* **18**, 43–78.

Homsy, G. M. 1987 Viscous fingering in porous media. *Annu. Rev. Fluid Mech.* **19**, 271–311.

Koval, E. J. 1963 A method for predicting the performance of unstable miscible displacement in heterogeneous media. *SPE J.* **3**, 145–155.

Lake, L. W. 1989 *Enhanced Oil Recovery*. Prentice Hall.

Lefloch, P. G. 2002 *Hyperbolic Systems of Conservation Laws: The Theory of Classical and Nonclassical Shock Waves*. Birkhauser.

Loggia, D., Rakotomalala, N., Salin, D. & Yortsos, Y. C. 1995 Evidence of new instability thresholds in miscible fluid flows. *Europhys. Lett.* **32**, 633–638.

Manickam, O. & Homsy, G. M. 1991 Fingering instabilities in a vertical displacement flows in porous media. *J. Fluid Mech.* **288**, 75–102.

Menon, G. & Otto, F. 2005 Dynamic scaling in miscible viscous fingering *Commun. Math. Phys.* **257**, 303–317.

Pelce, P. 1988 *Dynamics of Curved Fronts*. Academic.

Saffman, P. G. & Taylor, G. I. 1958 The penetration of a fluid into a porous medium or Hele-Shaw cell containing a more viscous fluid. *Proc. R. Soc. Lond.* A **245**, 312–329.

Shariati, M., Talon, L., Martin, J., Rakotomalala, N., Salin, D. & Yortsos, Y. C. 2004 Fluid displacement between two parallel plates: a non-empirical model displaying change of type from hyperbolic to elliptic equations. *J. Fluid Mech.* **519**, 105–132.

Smirnov, N. N., Nikitin, V. F., Maximenko, A., Thiercelin, M. & Legros, J. C. 2005 Instability and mixing flux in frontal displacement of viscous fluids from porous media. *Phys. Fluids* **17**, 084102.

Tanveer, S. 2000 Surprises in viscous fingering. *J. Fluid Mech.* **409**, 273–308.

Todd, M. R. & Longstaff, W. J. 1972 The development, testing, and application of a numerical simulator for predicting miscible flood performance. *J. Petrol. Tech.* **24**, 874–882.

Wooding, R. A. 1969 Growth of fingers at an unstable diffusing interface in a porous medium. *J. Fluid Mech.* **39**, 477–495.

Yang, Z. M. & Yortsos, Y. C. 1998 Effect of no-flow boundaries on viscous fingering in porous media of large aspect ratio. *SPE J.* **3**, 285–292.

Yang, Z. M., Yortsos, Y. C. & Salin, D. 2002 Asymptotic regimes in unstable miscible displacements in random porous media. *Adv. Water Resour.* **25**, 885–898.

Yortsos, Y. C. 1995 A theoretical analysis of vertical equilibrium. *Transport in Porous Media* **18**, 107–129.

Zimmerman, W. B. & Homsy. G. M. 1991 Viscous fingering in miscible displacements: unification of effects of viscosity contrast, anisotropic dispersion, and velocity dependence of dispersion on nonlinear finger propagation. *Phys. Fluids* A **4**, 2348–2359.